The Meteoritical Society

Meteoritics & Planetary Science 45, Nr 1, 123–134 (2010)
doi:10.1111/j.1945-5100.2009.01011.x

Analysis of ordinary chondrites using powder X-ray diffraction: 1. Modal mineral abundances

Tasha L. DUNN[1#*], Gordon CRESSEY[2], Harry Y. McSWEEN Jr.[1], and Timothy J. McCOY[3]

[1]Department of Earth and Planetary Sciences, Planetary Geosciences Institute, University of Tennessee, Knoxville, Tennessee 37920, USA
[2]Department of Mineralogy, The Natural History Museum, London SW7 5BD, UK
[3]Department of Mineral Sciences, National Museum of Natural History, Smithsonian Institution, Washington, D.C. 20013, USA
#Present address: Department of Geography-Geology, Illinois State University, Normal, Illinois 61761, USA
*Corresponding author. E-mail: tldunn@ilstu.edu

(Received May 28, 2008; revision accepted September 1, 2009)

Abstract–Powder X-ray diffraction (XRD) is used to quantify the modal abundances (in wt%) of 18 H, 17 L, and 13 LL unbrecciated ordinary chondrite falls, which represents the complete petrologic range of equilibrated ordinary chondrites (types 4–6). The XRD technique presents an effective alternative to traditional methods for determining modal abundances, such as optical point counting and electron microprobe phase (EMP) mapping. The majority of chondrite powders in this study were previously prepared for chemical characterization from 8 to 20 g of material, which is consistent with the suggested mass (10 g) necessary to provide representative sampling of ordinary chondrites. Olivine and low-Ca pyroxene are the most abundant phases present, comprising one-half to three-fourths of total abundances, while plagioclase, high-Ca pyroxene, troilite, and metal comprise the remaining XRD-measured mineralogy. Pigeonite may also be present in some samples, but it is fitted using a high-Ca pyroxene standard, so exact abundances cannot be measured directly using XRD. Comparison of XRD-measured abundances with calculated Cross, Iddings, Pirsson, Washington (CIPW) normative abundances indicates that systematic discrepancies exist between these two data sets, particularly in olivine and high-Ca pyroxene. This discrepancy is attributed to the absence of pigeonite as a possible phase in the CIPW normative mineralogy. Oxides associated with pigeonite are improperly allocated, resulting in overestimated normative olivine abundances and underestimated normative high-Ca pyroxene abundances. This suggests that the CIPW norm is poorly suited for determining mineralogical modal abundances of ordinary chondrites.

INTRODUCTION

Ordinary chondrites are not only the most abundant type of meteorite (representing more than 80% of all observed falls), but are also among the solar system's most primitive material. Most aspects of these meteorites have been thoroughly characterized, from bulk chemical (Kallemeyn et al. 1989; Jarosewich 1990) and isotopic compositions (Clayton et al. 1991) to mineral chemistry (e.g., Keil and Fredriksson 1964; Rubin 1990) and metamorphic petrology (Van Schmus and Wood 1967; Dodd 1969; McSween et al. 1988). However, our understanding of ordinary chondrite formation and parent-body processes has been hampered by an inability to determine precise abundances of the minerals that comprise them. Few credible determinations of phase abundances in ordinary chondrites exist because of the difficulty associated with quantifying modal abundances of fine-grained samples.

Modal mineralogy is traditionally determined using optical point counting. Although it is an established technique, optical point counting is better suited for samples that contain large grains, as small grains are difficult to identify. An energy dispersive spectrometer (EDS) phase-mapping technique (Taylor et al. 1996), which detects, measures, and analyzes phases present in

a backscattered electron image has been applied to ordinary chondrites (Gastineau-Lyons et al. 2002). The EDS phase-mapping technique with the electron microprobe is well-suited for determining the modal abundances of 2D slices of material (i.e., thin sections) at a precision that is user-dependent. Such 2D slices, however, may not be representative of entire samples. This method is also time-consuming (5–7 1000×1000 μm fields per hour), particularly if multiple determinations are required. Quantification of a large number of modal abundances may be better accomplished using a less time-consuming method, which measures a more representative sample of the bulk material.

Powder X-ray diffraction (XRD) provides a viable alternative to traditional modal analyses. Cressey and Schofield (1996) developed a method for determining modal abundances using powder XRD. This technique uses a position-sensitive detector (PSD), which allows for rapid collection of XRD patterns. Phase quantification can be carried out on patterns acquired in as little as 5 min (Batchelder and Cressey 1998), although longer count times are required for complex multiphase mixtures. Most complex samples require as little as 60 min of counting. Unlike traditional modal analyses (in which less abundant phases are difficult to quantify), well crystalline phases can often be detected at abundances as low as 1 wt%. XRD is also non-destructive (although samples are powdered, material is preserved during analysis) and can be used effectively on small volumes of material (approximately 1–2 mm^3). Accuracy is dependent on several factors, the most significant of which being standard matching. Bland et al. (2004) suggested phase abundances can be determined within an accuracy of ± 2 wt%, provided well-matched standards are available.

This powder XRD technique was first applied to quantification of ordinary chondrite modal abundances by Menzies et al. (2005), who determined the modes of six unequilibrated (relatively unaltered) type 3 ordinary chondrites and three equilibrated (thermally metamorphosed) type 4–6 ordinary chondrites (Van Schmus and Wood 1967). The success of the Menzies et al. (2005) study indicated that powder XRD could be used effectively on a much larger scale. In this study, we have quantified the modal abundances of 18 H, 17 L, and 13 LL ordinary chondrite samples, which together represents the complete petrologic range of equilibrated ordinary chondrites (types 4–6). In this paper, we introduce the XRD technique, report the modal abundances of all 48 ordinary chondrite samples, and compare our results with modal and normative ordinary chondrite abundances determined in previous studies (e.g., Gastineau-Lyons et al. 2002; McSween et al. 1991).

Because the only ordinary chondrites abundances available prior to this study were calculated from Cross, Iddings, Pirsson, Washington (CIPW) norms (McSween et al. 1991), this study represents the first statistically significant sampling of measured ordinary chondrite modal abundances. The modal data gathered here has many applications, one of the most useful being to improve our understanding of ordinary chondrite parent-body formation. In a companion paper, "Analysis of ordinary chondrites using powder X-ray diffraction: 2. Applications to ordinary chondrite parent-body processes" (this issue), we use our ordinary chondrite modal abundances, along with geochemical data from electron microprobe analysis, to address the questions of oxidation state and peak temperatures in ordinary chondrite parent asteroids in an attempt to develop a more thorough geochemical model of ordinary chondrite parent-body formation.

METHODOLOGY

Samples

A total of forty-eight ordinary chondrite samples representing each of the ordinary chondrites groups (H, L, and LL) and petrologic categories 4–6 (Van Schmus and Wood 1967) were selected for analysis (Table 1). Unequilibrated (type 3) chondrites are not included in this study, as modal abundances of type 3 chondrites were determined using powder XRD by Menzies et al. (2005), who examined the issue of redox state in the unequilibrated ordinary chondrites. To ensure that samples represented a single petrographic type, visibly polymict samples were excluded from the study, and only unbrecciated falls with minimal terrestrial weathering were selected for analysis. Terrestrial weathering of olivine often yields small (approximately 0.1 μm) crystals of serpentine and iron oxides, which produce a XRD-amorphous background (G. Cressey, personal communication). Representative powders of 37 of these samples were originally prepared for bulk chemical analysis by E. Jarosewich as part of the Smithsonian Institution's Analyzed Meteorite Powder Collection (chemical analyses published by Jarosewich 1990). Small chips (0.1–0.5 g) of the remaining 11 chondrites were acquired from the Natural History Museum (NHM) in London and the Smithsonian Institution. Samples obtained from the NHM were powdered on-site by museum personnel, while samples from the Smithsonian Institution were prepared for analysis at the University of Tennessee. These samples were ground with mortar and pestle to an approximate grain size of 35 μm. This grain size is necessary to provide a smooth surface for XRD experiments, which

Table 1. Chondrites analyzed in this study using powder X-ray diffraction.

Sample	Class	Source	Sample	Class	Source	Sample	Class	Source
Benares (a)	LL4	NHM[a]	Atarra	L4	AMPC	Farmville	H4	AMPC
Greenwell Springs	LL4	AMPC[b]	Bald Mountain[d]	L4	AMPC	Forest Vale	H4	AMPC
Hamlet	LL4	NHM	Rio Negro	L4	AMPC	Kabo	H4	AMPC
Witsand Farm	LL4	NHM	Rupota	L4	AMPC	Marilia[d]	H4	AMPC
Aldsworth	LL5	NHM	Ausson	L5	SI	São Jose do Rio Preto	H4	AMPC
Alat'ameem	LL5	NHM	Blackwell	L5	SI	Allegan	H5	AMPC
Olivenza	LL5	NHM	Cilimus	L5	AMPC	Ehole	H5	AMPC
Paragould	LL5	NHM	Guibga[d]	L5	AMPC	Itapicuru-Mirim[d]	H5	AMPC
Tuxtuac	LL5	SI[c]	Mabwe-Khoywa	L5	AMPC	Lost City	H5	AMPC
Bandong	LL6	AMPC	Malakal	L5	AMPC	Pribram	H5	AMPC
Cherokee Spring	LL6	AMPC	Messina	L5	AMPC	Schenectady	H5	AMPC
Karatu	LL6	AMPC	Apt	L6	AMPC	Uberaba	H5	AMPC
Saint-Severin	LL6	AMPC	Aumale	L6	AMPC	Andura	H6	AMPC
			Karkh	L6	AMPC	Butsura[d]	H6	AMPC
			Kunashak	L6	AMPC	Canon City	H6	AMPC
			Kyushu	L6	AMPC	Chiang Khan	H6	SI
			New Concord[d]	L6	AMPC	Guareña	H6	AMPC
						Ipiranga	H6	AMPC

[a]Natural History Museum, London, UK.
[b]Smithsonian Institution's analyzed meteorite powder collection.
[c]Smithsonian Institution—sample chip, not part of the analyzed meteorite powder collection.
[d]Counts acquired for 600 min.

is important for minimizing preferred orientation effects and microabsorption (beam attenuation because of surface roughness), as demonstrated by Batchelder and Cressey (1998).

The presence of Fe–Ni metal in a sample can hinder XRD analyses because it tends to sink into less dense silicate material during sample preparation (Menzies et al. 2005). As a result, XRD-derived metal abundances may not represent the actual abundance of metal in a sample. To resolve this problem, Menzies et al. (2005) magnetically separated metal from the silicate portion of each powdered meteorite sample prior to analysis and weighed both fractions to determine the wt% metal present. XRD-derived silicate abundances were then re-proportioned to account for amount of metal in a given sample. Fe–Ni metal in most samples analyzed in this study was removed and weighed by Jarosewich (1990) prior to our acquisition of the samples. In all other samples, Fe–Ni metal was removed magnetically and weighed following procedures outlined by Menzies et al. (2005).

The availability of sample material is a critical aspect of meteorite analysis, as the amount is usually limited. The majority of chondrite powders in this study were originally prepared by Eugene Jarosewich from 8 to 20 g of material, which is in line with the amount of material (10 g) required to provide a representative sampling of ordinary chondrites (Keil 1962). Less than 1 g of the original material was used for each XRD analysis. For chondrites not prepared as part of the Jarosewich (1990) study, availability of material was limited, and only small amounts (0.1–0.5 g) could be obtained. This may not be enough material to provide accurate modal mineralogies, and it is possible that these powders may not be as representative as those prepared by Jarosewich (1990). However, these samples were necessary to ensure that the H, L, and LL ordinary chondrite groups were equally represented. Powders were measured as thin section smears. Although the volume of material used in a thin smear is small (approximately 1–2 mm^3), this amount is sufficient to accurately measure modal mineralogies of ordinary chondrites. Modal heterogeneity in the CI meteorite Orgueil was investigated by Bland et al. (2004), who used XRD to measure 10 different aliquots of Orgueil in a micro-well with a volume (0.07 mm^3) that is significantly lower than that of a thin smear. The average mineralogy of these 10 aliquots was the same as modal mineralogy obtained using a standard well with a volume of 180 mm^3 (Bland et al. 2004). In this study, two different thin smears of the L5 chondrite Guibja were analyzed, one for 600 min and the other for 60 min. All phase abundances agree within 1 wt% except for olivine, which correlates within 2 wt%.

X-ray Diffraction

The XRD data were collected using an INEL-curved PSD (INL, Arteny, France) at the NHM in London. With this PSD, diffracted intensity is measured simultaneously at all angles, around an arc of

approximately 120° 2θ, resulting in rapid data collection. The angular range was calibrated using NIST silicon (SRM640) standard powder and the linearization of the detector was performed using a least-squares cubic spline function, resulting in an output array of 4017 channels each of 0.031° 2θ. Experimental configurations in this study are similar to those implemented by Bland et al. (2004) and Menzies et al. (2005). Samples were radiated using CuKα1 radiation, which was selected from the primary beam using a single-crystal Ge111 monochromator (Nonius, Bruker AXS, Madison, WI). Post-monochromator slits were used to restrict the beam size to 0.24 × 3.0 mm. Diffraction patterns were recorded in reflection geometry from the sample smear surface, which was set at an angle 7.5° to the incident beam. Because the detector remains fixed, the only movement is the sample itself, which spins slowly in its own plane. The absence of movement allows for very precise reproducibility of geometry from one sample to the next.

Powdered samples were analyzed on a single-crystal quartz substrate cut at an angle to prevent Bragg reflection, resulting in "zero background." Using this substrate, diffraction patterns can be obtained from very small sample volumes if necessary. Immediately prior to analysis, a portion of each powdered sample was placed on the substrate and a drop of acetone was added to allow the sample to be spread in situ with a needle point to form a thin smear of uniform thickness (approximately 30–40 μm). Acetone, which quickly evaporates, does not contaminate the sample or alter the XRD pattern. After preparation, we acquired counts on most samples for 60 min. A few samples were analyzed overnight, acquiring counts for a total of 600 min. Although accurate phase quantification can be carried out on patterns acquired in as little as 5 min (Batchelder and Cressey 1998), longer count times are required for complex multiphase mixtures, such as the ordinary chondrites analyzed in this study. Longer count times ensure that peak intensities are recorded accurately and that the ratio of background noise to peaks is reduced, thus improving resolution and detection limits for phases present in small abundances. Silicon was used as an external calibration standard, as described by Cressey and Schofield (1996).

Fitting Procedure

In the fitting procedure developed by Cressey and Schofield (1996), modal abundances are determined by fitting peak intensities of a mineral standard to those present in a mixture. The intensity of the whole-pattern standard phase is decreased by a factor equal to the intensity of that phase in the mixture and then subtracted, effectively removing that component from the mixture pattern. This procedure is repeated until all phases have been removed. The percentages of phases determined by this technique are termed "percentages of fit." Figure 1 shows representative XRD patterns of the LL4 chondrite Greenwell Springs. The measured pattern is the actual XRD pattern acquired in this study, whereas the calculated pattern (offset by 1000 counts for clarity) is a composite of all fitted standards at their appropriate proportions. The calculated Greenwell Springs pattern is a composite of 4.4% Fo_{60}, 30.5% Fo_{70}, 18.8% Fo_{80}, 23.4% enstatite, 6.8% diopside, 9.3% anorthite, and 6.9% troilite. The residual pattern is the measured pattern minus the calculated pattern. A zero residual indicates that all phases have been accounted for in the fitting procedure. Some intensity may remain in the residual because of slight differences in solid solution between the standards and the sample phases. Such residuals show up as paired negative–positive deviations in the residual. In other cases, a strong diffraction peak of a phase may be enhanced in the standard or in the sample owing to preferred orientation in the mount, and this extra intensity will show in the residual. However, because the whole pattern is used in the total fitting rather than just the main diffraction peaks, which is the practice used by most other methods employing scanning diffractometers, a strong peak can be excluded from the fitting procedure without affecting the final quantification result. These basic rules for assessing phase quantities

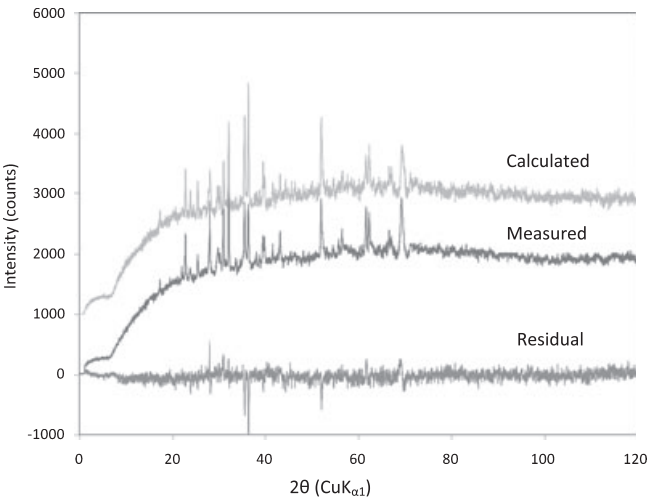

Fig. 1. Measured, calculated, and residual X-ray diffraction patterns for Greenwell Springs (LL4). The measured pattern is the actual X-ray diffraction pattern acquired in this study, whereas the calculated pattern (offset by 1000 counts for clarity) is a composite of all fitted standards at their appropriate proportions. The calculated Greenwell Springs pattern is a composite of 4.4% Fo_{60}, 30.5% Fo_{70}, 18.8% Fo_{80}, 23.4% enstatite, 6.8% diopside, 9.3% anorthite, and 6.9% troilite. The residual pattern is the measured pattern minus the calculated pattern. A zero residual indicates all phases have been accounted for in the fitting procedure.

from multiphase patterns have been addressed and demonstrated by Cressey and Schofield (1996).

In previous studies (e.g., Bland et al. 2004; Menzies et al. 2005) an ideal fit (i.e., all phases are accounted for) was indicated by a total fit of 100%, because the irradiated volumes of sample and standard phases were identical. This is not the case in this study, as the amount of chondrite powder available was insufficient to fill 1-mm-deep wells (180 mm^3 of material required). Instead, diffraction patterns of the chondrites in this study were recorded from thin smears, which require only 1–2 mm^3 of material, while standard patterns were determined from powders in 1-mm-deep wells. As a result, the irradiated volume of the samples is less than that of the standards, and consequently a 100% total fit is not achieved, even after all standard phases have been subtracted. This does not present a problem because the fitting procedure actually measures ratios of phases present in a sample, and therefore the volume of the standards and the volume of the sample need not be equal. However, the standard patterns must form an internally consistent data set with correct whole-pattern intensities relative to each other. This was achieved by recording the standards under identical conditions in the same volume deep well mounts. As fitting each sample with the standard patterns determines the relative proportions of phases present, the fit proportions can simply be normalized to 100% after the total fit has been performed. Total fits vary among samples as a result of small differences between sample volumes, which cannot be avoided when preparing thin smears. Because the sum of each sample's percentage of fit is unknown prior to fitting, a degree of uncertainty is added to the fitting procedure. The accuracy of each fit can be confirmed by examining residual XRD patterns, which should have near-zero residual counts.

Actual weight percentages of each mineral present are determined by correcting for the deadtime of the detector and for the mass absorption coefficient (μ/ρ). The deadtime correction is made by applying a multiplication factor of $100/(100\text{-}x)$, where x is the percentage deadtime. The mass absorption coefficient is different for each mineral (Batchelder and Cressey 1998). Minerals with low absorption, such as plagioclase, when in a mixture with higher-absorbing phases, will be underestimated by the fit relative to its actual wt%. Conversely, minerals with high absorption (e.g., forsterite-rich olivine) will be overestimated by the fit. Using compositional data, the mass absorption coefficient for each mineral was calculated from the weighted average of the mass absorption coefficients of its constituent elements, from values given in *International Tables for Crystallography*. Using the pattern-fit fraction of a single phase and the calculated mass absorption coefficients for each mineral in the mixture, the actual weight percentage of each mineral can be determined (Batchelder and Cressey 1998). (We refer the reader to Bland et al. 2004 for a detailed discussion of the conversion from XRD percentage fit to final wt%.) Weight percentages can be converted to volume percents if the density of each mineral phase is known. In this study, all results are presented in weight percentage to allow for comparison with previously calculated normative and measured modal abundances (McSween et al. 1991 and Gastineau-Lyons et al. 2002, respectively).

The detection limits for any particular phase will depend on many factors, such as the scattering power for X-rays (i.e., whether the phase is a good diffractor or not), the state and perfection of its crystallinity, the particle size, and the total matrix absorption characteristics. For well-crystalline phases these can often be detected and quantified at the 0.5–1% level. For the final quantification results, structural inhomogeneities, the degree of near-matching of standards, and any uncertainties in the assumed phase chemistries (leading to errors in the applied absorption corrections) will result in compounded errors. However, blind tests on known mixtures and exact-match standards (e.g., Madsen 1999; Madsen et al. 2001) demonstrate that the powder XRD method yields quantitative results to within ~1% of the actual proportions. Many other complex multiphase mixtures have now been quantified at the NHM in London using this method, and in such cases (where less-perfect, but near-matching of standards was achieved), the phase quantification results obtained are commonly within 2–3% of the actual values present. This situation can always be improved, given time, as a more comprehensive choice of standards are sought and characterized.

Standard Selection

Olivine abundances were determined using a series of olivine standards, with compositions ranging from Fo_{60} to Fo_{100}. However, most olivine was fitted using only the Fo_{70} and Fo_{80} standards, because they provide the best compositional match for olivine in the ordinary chondrites. Usage of the standards was not restricted to these two compositions, and many samples were fitted using two or more olivine standards. The range of olivine standards used in this study is consistent with olivine compositions in ordinary chondrites, which range from Fo_{84} in H chondrites to Fo_{68} in LL chondrites (Brearley and Jones 1998; and references therein). All low-Ca pyroxene abundances were determined using an enstatite standard with a composition of $En_{86}Fs_{12}Wo_3$. The Fs content of this standard is slightly lower than

that of typical orthopyroxene in ordinary chondrites, which ranges from $Fs_{14.5\text{-}18}$ in H chondrites, from $Fs_{19\text{-}22}$ in L chondrites, and from $Fs_{22\text{-}26}$ in LL chondrites (Brearley and Jones 1998; and references therein). High-Ca pyroxene abundances were determined using a diopside standard with a composition of $En_{47}Fs_6Wo_{47}$. In ordinary chondrites, high-Ca pyroxene is diopsidic in composition, with an average Wo content of approximately 45 and mean Fs contents ranging from Fs_7 to $Fs_{8.5}$ to Fs_{10} in the H, L, and LL groups (Brearley and Jones 1998; and reference therein). Therefore, the diopside standard used in this study is a good compositional match for high-Ca pyroxene in ordinary chondrites. Plagioclase, which is typically albitic (An_{10}–An_{12}) in ordinary chondrites (Brearley and Jones 1998), was fitted using a pure anorthite standard. Labradorite ($An_{50\text{–}70}$), which is a better compositional match for ordinary chondrites, was initially used to determine plagioclase compositions. However, XRD pattern fittings using the labradorite standard yielded plagioclase abundances >15 wt%, much higher than normative abundances (McSween et al. 1991), microprobe-measured abundances (Gastineau-Lyons et al. 2002), and our own optical observations. Consequently, anorthite, the only other available plagioclase standard, was used to determine abundances.

Because the composition of a mineral affects peak positions and peak intensities, an error in fitting is expected when a standard composition differs from the actual composition present. In orthopyroxene, peak positions of the 0k0 and hkl peaks shift to lower angles with increasing Fe, while the h00, 001, and h01 peaks remain in similar positions for all compositions. Changes in Fe content also alter peak intensities because the number of Fe atoms in the Mg sites of a structure affect X-ray scattering. Determining the fit becomes more problematic when the enstatite-ferrosilite solid-solution is far from the standard composition, as in the case of the LL chondrites. The same is also true for the diopside-hedenbergite series, and the largest compositional difference is again in the LL chondrites. The XRD pattern is also affected by the structural state of pyroxene (monoclinic vs. orthorhombic). To more accurately account for the presence of clinoenstatite (monoclinic) intergrowths in type 4 and 5 chondrites, both clinoenstatite and orthoenstatite standards would be required.

In plagioclase, the intensity of the main peak (31° 2θ) is not especially affected by compositional variations. However, XRD patterns of plagioclase are likely to be affected by structural state (i.e., Al-Si order/disorder). Anorthite is fully ordered (an equal number of Si and Al atoms alternate with regularity), while labradorite has a complex intermediate structure, which likely consists of alternating lamellae of albite and anorthite (Deer et al. 1992). Although the anorthite standard is a poor compositional match for ordinary chondrites, it appears to provide a better structural match than the labradorite standard. Using anorthite rather than labradorite does result in an additional error when correcting for mass absorption (μ/ρ anorthite, 52.7; μ/ρ labradorite, 47.3). Assuming a constant XRD % fit, using the anorthite standard increases final plagioclase abundances by approximately 1 wt%.

Because only a limited compositional range of standards was available in this study, error cannot be avoided, especially when standards differ significantly from measured compositions. The largest source of error is likely associated with fitting of pyroxenes, particularly in the LL chondrites, where standard compositions are furthest from measured compositions. Additional error also results from the plagioclase fitting, as compositional differences between the standard and measured values introduce a small error when determining final modal abundances. Future XRD studies of ordinary chondrites would benefit from an expanded mineral library, consisting of a wide compositional range of pyroxene and plagioclase standards, much like the existing olivine library.

RESULTS

Application to Ordinary Chondrite Mineralogy

To test the accuracy of the XRD method in mixtures with compositions similar to ordinary chondrites, we used the full pattern fitting procedure (Cressey and Schofield 1996) to determine modal abundances of five powder mixtures (prepared by T. J. McCoy at the Smithsonian Institution) consisting of varying proportions of plagioclase ($An_{11}Ab_{84}$), low-Ca pyroxene ($En_{78}Fs_{20}Wo_1$), high-Ca pyroxene ($En_{47}Fs_8Wo_{45}$), and olivine (Fo_{92}). These compositions are representative of the major mineral phases present in ordinary chondrites. To ensure consistency with our ordinary chondrite fittings, these unknown patterns were fitted using the same standards used to fit the ordinary chondrites. Table 2 compares XRD-derived modal abundances of the unknown mixtures with measured abundances, while Table 3 lists the compositions of standards used in this study. Overall, all XRD-derived phases are within ± 2.2 wt% of actual abundances, suggesting that, because the standards used are imperfect matches to the phases in the mixtures, the uncertainty of ordinary chondrite mineral abundances determined in this study is likely to be similar (i.e., to within about 2 wt% of the actual values).

Table 2. X-ray diffraction (XRD)-measured modal abundances of five silicate powder mixtures.

Composition of powder mixture[a]	Mineral phase	XRD % fit[b]	Deadtime correction[c]	μ/ρ[d]	XRD wt%
$OLV_{40}LCP_{49}HCP_{11}$					
	Forsterite 92	0.45	1.06	48.6	38.2
	Enstatite	0.65	1.09	53.4	50.1
	Diopside	0.15	1.05	63.3	11.6
$LCP_{50}HCP_{50}$					
	Enstatite	0.80	1.09	53.4	52.2
	Diopside	0.90	1.05	63.3	47.8
$LPC_{85}HCP_{15}$					
	Enstatite	0.90	1.09	53.4	84.7
	Diopside	0.15	1.05	63.3	15.3
$OLV_{80}LCP_{9}HCP_{2}PLG_{10}$					
	Forsterite 92	1.60	1.06	48.6	79.7
	Enstatite	0.20	1.09	53.4	10.0
	Diopside	0.00	1.05	63.3	0.0
	Anorthite	0.20	1.00	52.7	10.3
$OLV_{70}LCP_{30}$					
	Forsterite 92	0.80	1.06	48.6	71.1
	Enstatite	0.30	1.09	53.4	28.9

[a]Phases are reported in wt%; OLV, olivine; LCP, low-Ca pyroxene; HCP, high-Ca pyroxene; PLG, plagioclase.
[b]Raw fit data before corrections are made.
[c]Multiplication factor of $100/(100\text{-}x)$, where x is the percentage deadtime.
[d]Mass absorption coefficient (linear absorption coefficient/density).

Table 3. Compositions of standards used in this study.

Mineral	Composition
Olivine	Fo_{60}, Fo_{70}, Fo_{80}, Fo_{92}, Fo_{100}
Low-Ca pyroxene	$En_{86}Fs_{12}Wo_3$
High-Ca pyroxene	$En_{47}Fo_6Wo_{47}$
Plagioclase	An_{100}
Troilite	FeS (63.5 wt% Fe)

Modal Mineralogy

Olivine, low- and high-Ca pyroxene, plagioclase, and troilite were identified in all samples using the PSD-XRD method. Abundances of all XRD-measured silicate phases, along with metal abundances from bulk chemical analyses (Jarosewich 1990), are presented in Table 4. Olivine is the most abundant phase present, with abundances ranging from 29.1 to 57.2 wt%. Average olivine abundances increase from 33 wt% in the H chondrites to 51.1 wt% in the LL chondrites. Low-Ca pyroxene is the second most common phase present. Low-Ca pyroxene abundances range from 17.6 to 28.2 wt%, and average low-Ca pyroxene abundances decrease from 25.6 wt% in the H chondrites to 21.2 wt% in the LL chondrites. Plagioclase, high-Ca pyroxene, troilite, and metal comprise the remaining XRD-measured mineralogy of each sample. Plagioclase is present at abundances ranging from 8.1 to 12.3 wt%, with an average abundance of 9.3 wt%. High-Ca pyroxene is present at abundances ranging from 5.1 to 10.7 wt%, and troilite comprises an average of 6.3 wt% of each sample. Average modal abundances and standard deviations of the H, L, and LL chondrites are listed in Table 5 and are presented in Fig. 2. Modal abundances of each sample (in wt% and XRD percentage fit) are provided as supplemental online material (Table S1).

Comparison of XRD Modal Abundances and Electron Microprobe Modal Abundances

Gastineau-Lyons et al. (2002) determined the modal abundances of three L and four LL ordinary chondrites using an EMP-mapping technique (Taylor et al. 1996), in which user-defined "windows" of the energy dispersive spectrum are used to identify phases present in a sample. Modal abundances of five samples analyzed by Gastineau-Lyons et al. (2002) were also measured in this study. These samples are Bald Mountain (L4), Greenwell Springs (LL4), Olivenza (LL5), Tuxtuac (LL5), and Saint-Séverin (LL6). Figure 3 compares the XRD-derived modal abundances of these five samples with abundances determined using the microprobe phase-mapping technique. The electron microprobe-measured Olivenza mode used here is an average of the two sets of abundances (based on two separate thin sections) reported in Gastineau-Lyons et al. (2002). Both sets of data are presented in weight percentage.

Comparison of XRD data and electron microprobe values yield two significant observations, the first of which being that XRD-measured high-Ca pyroxene abundances appear to include the pyroxene pigeonite (Fig. 3). Pigeonite ($Wo_{5\text{-}20}$) is compositionally and structurally similar to clinoenstatite, the monoclinic form of low-Ca pyroxene, and has been identified in ordinary chondrites (primarily in type 3) in previous studies (e.g., Keil 1978; McSween and Patchen 1989). A pigeonite standard was not available at the time this study was complete, so any pigeonite present in a sample would be fitted either as low-Ca pyroxene (using the enstatite standard) or as high-Ca pyroxene (using diopside). Because both pigeonite and diopside are monoclinic, we would expect pigeonite to be fitted as high-Ca pyroxene. Table 6 shows that a direct comparison between electron microprobe-measured diopside abundances and XRD-derived high-Ca pyroxene abundances yields discrepancies of 1.9–6.2 wt%. However when pigeonite, which was identified and measured using the EMP-mapping technique, is added to EMP-measured diopside abundances, these differences decrease significantly. In Bald Mountain

Table 4. X-ray diffraction-derived modal abundances of ordinary chondrites analyzed in this study.

Sample	Class	Olivine	Low-Ca pyroxene	High-Ca pyroxene	Plagioclase	Troilite	Metal	Other[b]
Farmville	H4	30.3	27.9	7.6	8.7	5.6	18.5	1.6
Forest Vale	H4	30.1	25.5	7.4	8.5	5.4	21.4	1.7
Kabo	H4	29.1	27.0	6.8	9.7	6.2	19.5	1.7
Marilia	H4	29.7	28.2	6.5	9.4	6.0	18.7	1.6
São Jose do Rio Preto	H4	29.8	26.4	8.2	9.4	6.8	17.8	1.6
Allegan	H5	30.1	26.5	7.2	8.2	6.6	19.8	1.7
Ehole	H5	34.7	26.2	7.1	8.1	4.6	17.8	1.6
Itapicuru-Mirim	H5	32.9	23.2	6.3	9.0	5.8	21.3	1.6
Lost City	H5	31.4	25.4	7.4	10.1	5.4	18.5	1.8
Pribram	H5	32.3	25.9	7.7	8.8	7.0	16.7	1.6
Schenectady	H5	35.7	24.8	6.2	8.9	5.7	16.9	1.7
Uberaba	H5	34.7	24.5	8.3	9.5	6.1	15.3	1.6
Andura	H6	36.2	26.8	5.1	8.8	5.9	15.5	1.8
Butsura	H6	34.1	27.2	5.9	8.4	4.1	18.5	1.8
Canon City	H6	35.0	23.8	6.0	8.5	6.1	18.8	1.8
Chiang Khan	H6	34.4	24.8	6.0	9.2	6.0	18.0[a]	1.6
Guareña	H6	39.9	21.5	4.7	9.3	4.8	18.2	1.7
Ipiranga	H6	34.3	25.3	6.3	9.1	6.5	16.9	1.6
Atarra	L4	39.9	21.0	10.7	9.8	7.8	8.7	1.6
Bald Mountain	L4	38.4	23.9	8.1	9.3	8.9	9.8	1.6
Rio Negro	L4	42.0	25.2	8.5	9.8	4.7	8.1	1.7
Rupota	L4	42.6	24.4	7.9	9.1	6.4	8.1	1.7
Ausson	L5	38.7	24.9	7.2	12.3	5.5	9.9[a]	1.5
Blackwell	L5	44.6	25.9	9.6	8.8	2.6	6.9[a]	1.6
Cilimus	L5	44.3	25.0	6.8	9.3	5.6	7.6	1.6
Guibga	L5	40.9	22.1	8.0	9.1	9.1	9.4	1.4
Mabwe-Khoywa	L5	42.2	24.8	6.1	9.2	8.3	7.8	1.6
Malakal	L5	41.8	23.2	8.1	9.3	7.4	8.8	1.4
Messina	L5	42.9	23.4	8.4	7.2	8.7	7.9	1.5
Apt	L6	40.0	22.7	8.2	9.4	10.3	7.8	1.6
Aumale	L6	42.4	21.5	7.8	8.9	8.9	8.9	1.6
Karkh	L6	43.4	22.5	7.8	9.0	7.2	8.6	1.6
Kunashak	L6	43.9	21.9	7.6	10.2	7.0	7.7	1.6
Kyushu	L6	43.4	20.1	8.2	9.3	9.3	8.2	1.4
New Concord	L6	44.7	21.6	8.8	10.0	5.0	8.4	1.5
Benares (a)	LL4	47.6	24.1	9.8	11.2	5.3	0.5[a]	1.6
Greenwell Springs	LL4	50.5	22.0	6.4	8.8	6.5	4.3	1.5
Hamlet	LL4	49.9	23.2	7.3	10.0	4.7	3.4[a]	1.6
Witsand Farm	LL4	50.8	20.9	6.8	8.7	4.2	7.1[a]	1.6
Aldsworth	LL5	52.1	21.1	6.6	9.0	4.8	4.8[a]	1.6
Alat'ameem	LL5	51.1	23.3	7.9	9.0	5.1	2.0[a]	1.6
Olivenza	LL5	51.0	21.9	6.8	9.4	6.3	3.0[a]	1.7
Paragould	LL5	49.4	19.9	6.7	10.3	4.9	7.2[a]	1.6
Tuxtuac	LL5	51.9	22.7	7.9	10.1	3.6	2.2[a]	1.6
Bandong	LL6	50.4	18.6	7.5	10.8	8.6	2.4	1.7
Cherokee Spring	LL6	51.2	19.1	6.6	10.1	8.1	3.3	1.5
Karatu	LL6	57.2	17.6	8.2	9.4	4.7	1.6	1.4
Saint-Severin	LL6	51.3	20.1	7.4	9.5	6.8	3.2	1.6

[a]Metal abundances measured in this study; all others are from Jarosewich (1990).
[b]Normative abundances of apatite, ilmenite, and chromite (McSween et al. 1991); Average abundances were used when individual norms were not available.

(L4) the discrepancy between XRD-derived high-Ca pyroxene and EMP-measured diopside decreases by 89% (from 6.2 to 0.7 wt%) when EMP-measured pigeonite and diopside abundances are combined (Table 6). The same is true for the remaining samples, in which the correlation between XRD and EMP

Table 5. Average X-ray diffraction-measured abundances and standard deviations[a].

Chondrite group	No. samples	Olivine	Low-Ca pyroxene	High-Ca pyroxene	Plagioclase	Troilite
H4	5	29.8 (1.4)	27.0 (1.9)	7.3 (0.2)	9.1 (0.1)	6.0 (0.7)
H5	7	33.1 (2.0)	25.2 (1.1)	7.2 (0.7)	8.9 (0.7)	5.9 (0.8)
H6	6	35.7 (2.2)	24.9 (2.1)	5.7 (0.6)	8.9 (0.4)	5.6 (0.9)
L4	4	40.7 (1.9)	23.6 (1.8)	8.8 (1.3)	9.5 (0.4)	7.0 (1.8)
L5	7	42.2 (2.0)	24.2 (1.3)	7.7 (1.2)	9.3 (1.5)	6.8 (2.3)
L6	6	43.0 (1.6)	21.7 (0.9)	8.1 (0.4)	9.5 (0.5)	8.0 (1.9)
LL4	4	49.7 (1.5)	22.6 (1.4)	7.6 (1.5)	9.7 (1.2)	3.8 (1.0)
LL5	5	51.1 (1.1)	21.8 (1.4)	7.2 (0.7)	9.6 (0.6)	3.8 (0.9)
LL6	4	52.5 (3.1)	18.9 (1.0)	7.5 (0.6)	9.8 (0.7)	2.6 (1.8)

[a]Numbers in parentheses represent 1σ standard deviations

abundances of high-Ca pyroxene improves by 67% to 84%. These observations support the suggestion that pigeonite is fitted as high-Ca pyroxene. The exact amount of pigeonite in each sample cannot be determined, however, without a pigeonite standard.

Comparison of electron microprobe abundances with XRD abundances also appears to suggest that the microprobe phase-mapping technique agrees better with the XRD technique as the ordinary chondrites become more equilibrated. However, because only five samples are compared, this correlation may not be valid for a larger number of samples. Of the samples compared here, modal abundances in the type 4 chondrites Bald Mountain and Greenwell Springs show the largest disagreement with probe abundances. Modal olivine abundances in the type 4 chondrites are (on average) 5.8 wt% higher than probe abundances, while low-Ca pyroxene abundances are 2.1 wt% lower. Average XRD-derived plagioclase abundances are 2.3 wt% higher than EMP-measured abundances. In the type 5 chondrites, average XRD-derived olivine and low-Ca pyroxene abundances are within 2.5 wt% of probe abundances, while plagioclase abundances agree within 1.2 wt%. In St. Séverin (LL6), the most equilibrated chondrite examined by both techniques, all phases are within 1.1 wt% of probe values. These data do seem to suggest that the techniques agree better as chondrites become more equilibrated. This convergence at type 6 is not unexpected, as mineral phases become progressively more equilibrated and grain sizes increase with increasing petrologic type. Like optical point counting, fine-grained samples are more difficult to measure accurately using the EMP technique, so we would expect EMP-measured abundances to be more accurate in equilibrated samples. However, because the XRD technique measures powders rather than thin sections, grain size is not a factor, and we suggest that XRD-derived abundances of type 4 and 5 chondrites are more accurate than those determined using the EMP phase-mapping technique.

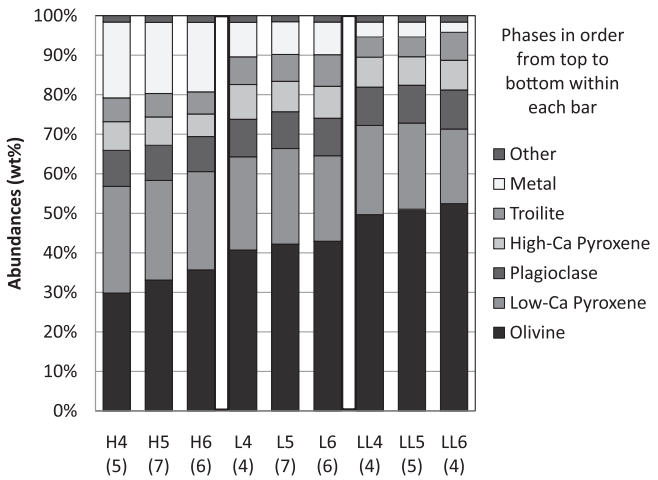

Fig. 2. Average X-ray diffraction-derived modal abundances (in wt%) of H, L, and LL ordinary chondrites for each petrologic type (4–6). Numbers in parentheses represent number of samples averaged.

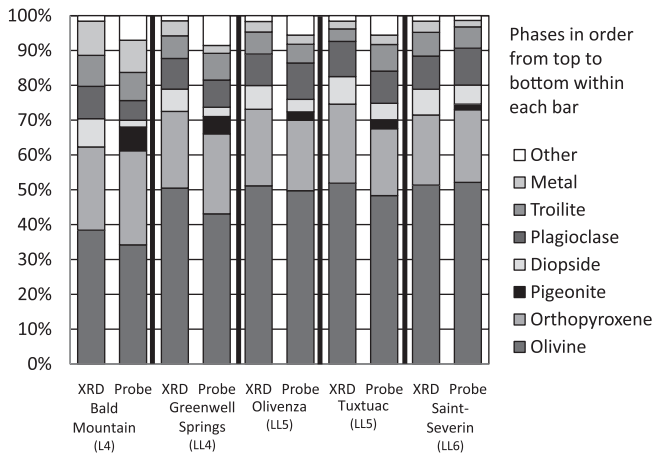

Fig. 3. Comparison of X-ray diffraction-derived modal abundances and electron microprobe-measured abundances (Gastineau-Lyons et al. 2002) of one L and four LL ordinary chondrites. Values are in wt%.

Table 6. Comparison of X-ray diffraction (XRD)-derived high-Ca pyroxene and electron microprobe phase (EMP)-measured diopside plus pigeonite[a].

		XRD	EMP		XRD	EMP	
Sample	Type	High-Ca pyroxene	Diopside	Absolute error	High-Ca pyroxene	Diposide + pigenoite	Absolute error
Bald Mountain	L4	8.1	2.0	6.1	8.1	8.8	0.7
Greenwell Springs	LL4	6.4	2.7	3.7	6.4	7.6	1.2
Olivenza	LL5	6.8	3.6	3.2	6.8	6	0.8
Tuxtuac	LL5	7.9	4.7	3.2	7.9	7.3	0.6
Saint-Severin	LL6	7.4	5.5	1.9	7.4	7.1	0.3

[a]Values are in wt%.

Comparison of XRD Modal Abundances and Normative Abundances

McSween et al. (1991) calculated CIPW normative mineral abundances of 27 H chondrites, 55 L chondrites, and 12 LL chondrites from bulk rock chemistries determined by Jarosewich (1990). Normative silicate mineralogy was calculated (as a set of anhydrous minerals) using the standard CIPW algorithm. As metal and sulfide minerals are not calculated as part of a CIPW norm, these minerals were physically measured, added to CIPW-calculated silicate abundances, and renormalized to 100%. Normative data for all but nine samples analyzed in this study are presented in McSween et al. (1991), allowing for a thorough comparison with modal data. Normative abundances cannot be calculated for the remaining nine samples because bulk chemical data are not available. Bulk chemical analyses are necessary to calculate norms properly, as a distinction between metallic Fe and Fe^{2+} must be made in the CIPW algorithm. On the basis of normative mineralogy, olivine is the most abundant phase present in all ordinary chondrite groups, followed by low-Ca pyroxene (enstatite), plagioclase, and high-Ca pyroxene (diopside).

Figure 4 compares modal and normative abundances of olivine, low-Ca pyroxene, high-Ca pyroxene, and plagioclase in 18 H, 15 L, and 6 LL chondrites. (As discussed in the previous section, high-Ca pyroxene abundances include any pigeonite that may be present.) Apatite, chromite, ilmenite, and metal (Table 4), which were not measured as part of this study, are not included in this comparison. Two L and seven LL chondrites, for which bulk compositions have not been measured, are not included in this comparison. Overall, modal low-Ca pyroxene and plagioclase are comparable with normative values (Fig. 4). Modal plagioclase abundances are within 1.5 wt% of normative abundances in all but three L chondrites (Ausson, Messina, and Aumale), and modal low-Ca pyroxene abundances agree within 0.2–3.4 wt% of normative abundances in all but four samples. There are systematic discrepancies, however, between XRD-measured and normative abundances of olivine and high-Ca pyroxene. XRD-derived olivine abundances are systematically lower than normative abundances by an average of 3 wt%, while XRD high-Ca pyroxene abundances are systematically higher by an average of 2.7 wt%.

The consistent disagreement between modal and normative abundances of olivine and diopside is likely a direct result of the way that CIPW norms are calculated, and these discrepancies suggest that CIPW norms are not well-suited for ordinary chondrites. The CIPW procedure calculates normative abundances by allocating measured oxides to a set of prescribed minerals. Not all minerals or solid solutions are represented by a CIPW norm, and if oxides are incorrectly combined or allocated, inaccurate normative abundances may result. The omission of pigeonite in the normative calculation suggests that this is the case in the normative abundances of ordinary chondrites. In a CIPW norm, all pyroxene is calculated as either diopside (high-Ca pyroxene) or enstatite (low-Ca pyroxene). Because pigeonite is not a possible phase, its associated oxides (CaO, FeO, and MgO) would be allocated to another mineral phase in the normative calculation. A likely possibility is olivine, whose normative abundances are determined using the same oxides found in pigeonite (primarily FeO and MgO). Because normative olivine abundances are systematically higher than XRD-derived olivine abundances (Fig. 4), it does appear that pigeonite is indeed being inappropriately allocated to olivine in the CIPW norm calculation. This error in calculation of normative olivine also explains the discrepancy between measured and normative diopside abundances. Because pigeonite is not a possible phase, XRD-derived high-Ca pyroxene abundances (which include pigeonite) are consistently higher than normative diopside. These observations indicate that CIPW normative calculation is not well-suited for ordinary chondrites, and we suggest that XRD-derived modal abundances are more representative of actual ordinary chondrite mineralogies.

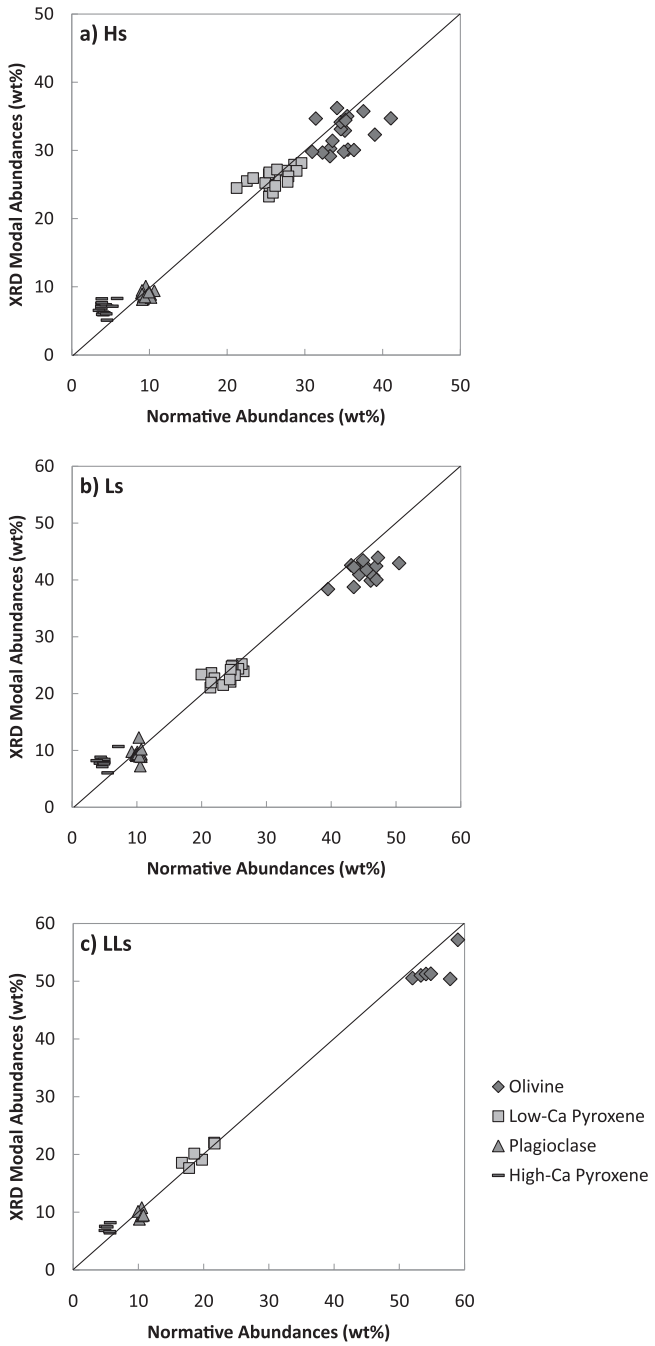

Fig. 4. Comparison of normative abundances (McSween et al. 1991) with X-ray diffraction-derived modal abundances in (a) H, (b) L, (c) LL ordinary chondrites. The diagonal lines represent a 1:1 normative to modal ratio.

CONCLUSIONS

We quantified the modal mineralogical abundances of 18 H, 17 L, and 13 LL equilibrated (type 4–6) ordinary chondrites using powder XRD. This XRD technique is a valuable analytical tool and is an effective alternative to traditional methods for determining modal abundances, which may not be well-suited for fine-grained samples. Our analysis of these samples yields the following conclusions:

1. Ordinary chondrites are comprised primarily of olivine and low-Ca pyroxene (50–75 wt% total), with some high-Ca pyroxene, plagioclase, metal, and troilite. Olivine abundances increase from the H to the LL chondrites, whereas low-Ca pyroxene and metal abundances decrease. High-Ca pyroxene, plagioclase, and troilite abundances are relatively consistent between the three ordinary chondrite groups. These conclusions reinforce those of previous mineralogic studies of ordinary chondrites.

2. Comparison of XRD-derived modal abundances with modal abundances measured using EMP mapping (Gastineau-Lyons et al. 2002) indicates that the monoclinic pyroxene pigeonite is fitted using the high-Ca pyroxene standard. This suggests that all XRD-derived high-Ca pyroxene abundances include both diopside and pigeonite (if present). The exact abundance of pigeonite, however, cannot be determined without a pigeonite standard.

3. Comparison of EMP-measured and XRD-derived modal abundances also suggests that both techniques correlate more closely with increasing petrologic type. Because only five samples were compared in this study, this correlation may not be valid for a larger number of samples. In petrologic types 4 and 5, mineral phases are less equilibrated and grain sizes are smaller. Because the EMP technique is sensitive to grain size while the XRD method is not, we suggest that XRD-derived abundances of type 4 and 5 chondrites are more accurate.

4. Normative abundances of olivine and high-Ca pyroxene, which are systematically higher and lower (respectively) than XRD-derived and EMP-measured abundances, can be explained by the absence of pigeonite in the CIPW norm calculation. Oxides associated with pigeonite (FeO and MgO) are incorrectly allocated to olivine, resulting in an overestimation of olivine and an underestimation of high-Ca pyroxene. Therefore, the CIPW norm is poorly suited for determining abundances of ordinary chondrites.

Acknowledgments—We would like to thank the Mineralogy Department at the Natural History Museum in London for the use of their facilities and for providing samples. The authors also thank the Smithsonian Institution for providing thin sections and powders of the majority of samples examined in this study. The authors are also grateful to Rhian Jones, Alex Ruzicka, and Adrian Brearley for their comments and suggestions, which have greatly improved this manuscript. This work

was supported by NASA through cosmochemistry grant NNG06GG36G to H. Y. M.

Editorial Handling—Dr. Adrian Brearley

REFERENCES

Batchelder M. and Cressey G. 1998. Rapid, accurate phase quantification of clay-bearing samples using a position sensitive X-ray detector. *Clays and Clay Minerals* 46:183–194.

Bland P. A., Cressey G., and Menzies O. N. 2004. Modal mineralogies of carbonaceous chondrites by X-ray diffraction and Mossbauer spectroscopy. *Meteoritics & Planetary Science* 39:3–16.

Brearley A. J. and Jones R. H. 1998. Chondritic meteorites. In *Planetary materials, reviews in mineralogy*, edited by Papike J. J. Washington, D.C.: Mineralogical Society of America. pp. 3-1–3-398.

Clayton R. N., Mayeda T. K., Goswami J. N., and Olsen E. J. 1991. Oxygen isotope studies of ordinary chondrites. *Geochimica et Cosmochimica Acta* 55:2317–2337.

Cressey G. and Schofield P. F. 1996. Rapid whole-pattern profile stripping methods for the quantification of multiphase samples. *Powder Diffraction* 11:35–39.

Deer W. A., Howie R. A., and Zussman J. 1992. *The rock-forming minerals*, 2nd edn. Essex: Addison Wesley Longman Limited. 696 p.

Dodd R. T. 1969. Metamorphism of the ordinary chondrites: A review. *Geochimica et Cosmochimica Acta* 33:161–203.

Gastineau-Lyons H. K., McSween H. Y. Jr., and Gaffey M. J. 2002. A critical evaluation of oxidation versus reduction during metamorphism of L and LL group chondrites, and implications for asteroid spectroscopy. *Meteoritics & Planetary Science* 37:75–89.

Jarosewich E. 1990. Chemical analyses of meteorites: A compilation of stony and iron meteorite analyses. *Meteoritics* 25:323–337.

Kallemeyn G. W., Rubin A. E., Wang D., and Wasson J. T. 1989. Ordinary chondrites: Bulk compositions, classification, lithophile-element fractionations, and composition-petrographic type relationships. *Geochimica et Cosmochimica Acta* 53:2747–2767.

Keil K. 1962. Quantitativ-erzmikroskopische Intergrationanalyse der Chondrite. *Chemie der Erde* 22:281–348.

Keil K. 1978. Studies of Brazilian meteorites XIV. Mineralogy, petrology, and chemistry of the Conquista, Minas Gerais, chondrite. *Meteoritics* 13:177–187.

Keil K. and Fredriksson K. 1964. The iron, magnesium, and calcium distribution in coexisting olivines and rhombic pyroxenes of chondrites. *Journal of Geophysical Research* 69:3487–3515.

Madsen I. C. 1999. Quantitative phase analysis round robin. *International Union of Crystallography Newsletter* 22:3–5.

Madsen I. C., Scarlett N. V. Y., Cranswick L. M. D., and Lwin T. 2001. Outcomes of the International Union of Crystallography Commission on Powder Diffraction round robin on quantitative phase analysis: Samples 1a and 1h. *Journal of Applied Crystallography* 34:409–426.

McSween H. Y. Jr. and Patchen A. 1989. Pyroxene thermobarometry in LL-group chondrites and implications for parent body metamorphism. *Meteoritics* 24:219–226.

McSween H. Y. Jr., Sears W. G., and Dodd R. T. 1988. Thermal metamorphism. In *Meteorites and the early solar system*, edited by Kerridge J. F. and Matthews M. S. Tucson: University of Arizona Press. pp. 102–113.

McSween H. Y. Jr., Bennett M. E., and Jarosewich E. 1991. The mineralogy of ordinary chondrites and implications for asteroid spectrophotometry. *Icarus* 90:107–116.

Menzies O. N., Bland P. A., Berry F. J., and Cressey G. A. 2005. Mossbauer spectroscopy and X-ray diffraction study of ordinary chondrites: Quantification of modal mineralogy and implications for redox conditions during metamorphism. *Meteoritics & Planetary Science* 40:1023–1042.

Rubin A. E. 1990. Kamacite and olivine in ordinary chondrites: Intergroup and intragroup variations. *Geochimica et Cosmochimica Acta* 54:1217–1232.

Taylor L. A., Patchen A., Taylor D. H. S., Chambers J. G., and McKay D. S. 1996. X-ray digital imaging and petrology of lunar mare soils: Data input for remote sensing calibrations. *Icarus* 124:500–512.

Van Schmus W. R. and Wood J. A. 1967. A chemical-petrologic classification for the chondrite meteorites. *Geochimica et Cosmochimica Acta* 31:747–765.

SUPPORTING INFORMATION

Additional Supporting Information may be found in the online version of this article:

Table S1. Detailed XRD fitting information and modal abundances of all ordinary chondrites analyzed in this study.

Please note: Wiley-Blackwell are not responsible for the content or functionality of any supporting materials supplied by the authors. Any queries (other than missing material) should be directed to the corresponding author for the article.